Enabling Autonomous Colonoscopy Intervention Using a Robotic Endoscope Platform

Qi Zhang, J. Micah Prendergast, Gregory A. Formosa, *Student Member, IEEE*
Mitchell J. Fulton, Mark E. Rentschler, *Senior Member, IEEE*

Abstract— ***Objective:*** **Robotic endoscopes have the potential to dramatically improve endoscopy procedures, however current attempts remain limited due to mobility and sensing challenges and have yet to offer the full capabilities of traditional tools. Endoscopic intervention (e.g., biopsy) for robotic systems remains an understudied problem and must be addressed prior to clinical adoption. This paper presents an autonomous intervention technique onboard a Robotic Endoscope Platform (REP) using endoscopy forceps, an auto-feeding mechanism, and positional feedback. M*ethods:* A workspace model is established for estimating tool position while a Structure from Motion (SfM) approach is used for target-polyp position estimation with the onboard camera and positional sensor. Utilizing this data, a visual system for controlling the REP position and forceps extension is developed and tested within multiple anatomical environments. *Results:* The workspace model demonstrates accuracy of 5.5% while the target-polyp estimates are within 5 mm of absolute error. This successful experiment requires only 15 seconds once the polyp has been located, with a success rate of 43% using a 1 cm polyp, 67% for a 2 cm polyp, and 81% for a 3 cm polyp. *Conclusion:* Workspace modeling and visual sensing techniques allow for autonomous endoscopic intervention and demonstrate the potential for similar strategies to be used onboard mobile robotic endoscopic devices. *Significance:* To the authors' knowledge this is the first attempt at automating the task of colonoscopy intervention onboard a mobile robot. While the REP is not sized for actual procedures, these techniques are translatable to devices suitable for *in vivo* application.**

***Index Terms*—Robotic Endoscope, Motion control, Visual Servoing, Visual tracking, Workspace model**

I. Introduction

COLORECTAL cancer (CRC) is the second most prevalent cancer in the United States, with approximately fifty thousand people dying from this disease every year [1]. CRC typically begins as polyps that grow slowly in the colon, however patients have a substantially increased chance of survival if these pre-cancerous polyps are removed at an early stage. A colonoscopy is the recommended screening method for CRC, allowing the gastroenterologist to examine and look for polyps and diseases within the colon by inserting a flexible colonoscope which has a small camera, light source, and several channels for irrigation, suction, air, and instrument tool port for biopsy. During the colonoscopy, the surgical instrument can pass through the colonoscope to biopsy tissue from the suspected polyp. The colonoscopy usually lasts 30 to 60 minutes, however, it may cause significant discomfort/pain to patients when the colonoscope advances along the tortuous path of the colon. To reduce the patient pain, swallowable pill-sized capsule endoscopes (CEs) are used as a less invasive screening method, but the passive movement of CEs leaves them with limited observation capabilities and the inability to implement

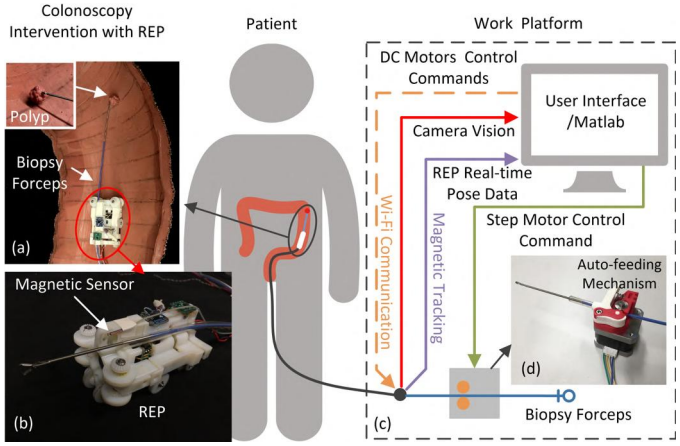

Fig. 1. Autonomous colonoscopy intervention system overview. (a) The Robotic Endoscope Platform (REP) carries the biopsy forceps to reach a polyp; (b) a magnetic sensor is attached on the REP to measure its pose; (c) the work platform that is placed outside the patient contains the auto-feeding mechanism and the user interface built in MATLAB; (d) the auto-feeding mechanism.

This research was supported in part by the National Science Foundation (NSF) (Grant Nos. 1849357). This research was also conducted with government support under and awarded by the Department of Defense, Air Force Office of Scientific Research, and National Defense Science and Engineering Graduate (NDSEG) Fellowship 32 CFR 168a. Mark Rentschler is a co-founder of Aspero Medical, Inc., a University of Colorado spin-out company that is focused on commercializing balloon overtube products for use in enteroscopy.

Q. Zhang is with the School of Mechanical Engineering, Southeast University, Nanjing 211189, China (e-mail: kichy_zq@163.com).

J. M. Prendergast, G. Formosa, M. Fulton, and M. Rentschler are with the department of Mechanical Engineering, University of Colorado, Boulder, CO, 80309 USA (e-mail: mark.rentschler@colorado.edu).

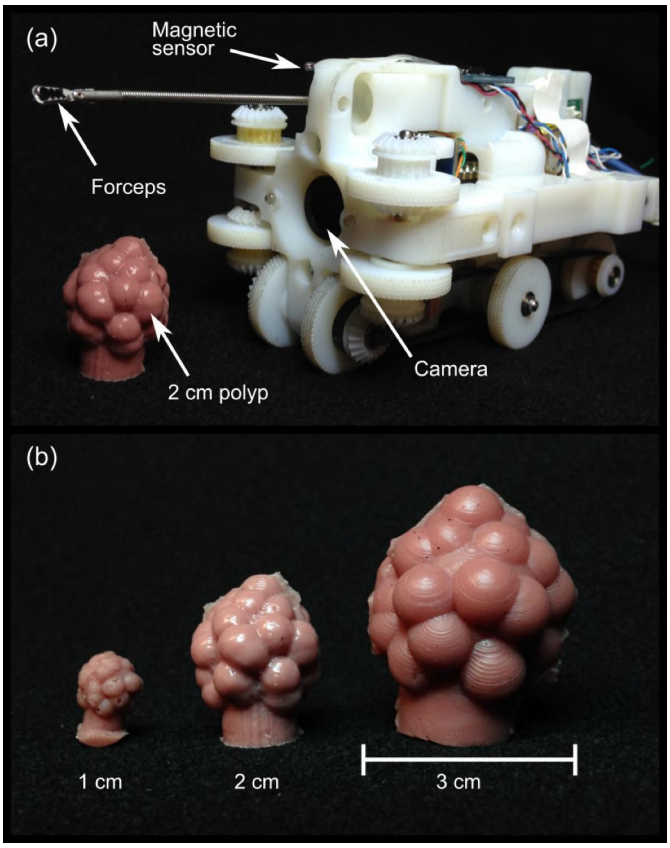

Fig. 2. Robotic Endoscope Platform (REP) is shown next to 2 cm diameter simulated polyp with forceps partly extended (A). The three different simulated polyps used in experimental testing are shown (B). The REP is a 2x robotic capsule endoscope platform (8x volume) [23]. Thus the polyps shown are twice the expected diameter in a patient.

therapeutic treatments [2, 3].

To achieve a more comprehensive examination strategy while also reducing patient discomfort during these screenings, robotic capsule endoscopes with active locomotion have been developed in recent years. These technologies include leg-like mechanisms [4-6], magnetically driven colonoscopes [7-10], worm-inspired robots [11-13], and wheeled platforms [14-16]. They have controllable movement and locomotion but are not available for commercial use due to their drawbacks such as slow movement, complex mechanism design, and safety concerns. What's more, while research towards these robotic endoscopes has focused on mobility and locomotion little work has been done towards applying these devices in colonoscopy intervention procedures such as removal of a suspected polyp.

In a traditional colonoscopy, the intervention is performed by an experienced endoscopist, and requires precise, flexible and fast operations of endoscopic surgical instruments. However, there are many difficulties in intervening within the colon, including lack of dexterity and unstable positioning. In the research field of robotic capsule endoscopy, various strategies for colonoscopy intervention have been proposed. Several micro modules for wireless capsule endoscopes were proposed for extracting target tissue samples, including rotational micro biopsy [17] and microbiopsy with torsion spring actuated microspike [18]. However, these are unable to reach a specific target tissue, to address this issue, an untethered and self-folding microgrippers on a magnetic capsule endoscope is designed for extracting tissue at a target location [19]. Similarly, a magnetically driven capsule endoscope with a fine needle is designed for capturing biopsy samples [20]. In addition to tissue removal, a wireless capsule endoscope is proposed for drug delivery at a target position [21]. Although these wireless capsule endoscopes are small enough for biopsy even in the small intestine, they only have one single biopsy function, moreover, the locomotion and target positioning accuracy needs to be substantially improved before clinical adoption.

The singular function of these biopsy capable devices is a critical limitation as there are many commercial endoscopic surgical instruments for different sizes and shapes of polyps in traditional colonoscopy, including various forceps, snares, needles, and retrieval nets [22]. The ability to use different instruments for different polyps is important for improving the success rate of colonoscopy intervention. It is reported that a magnetically driven robotic capsule reserved a channel for endoscopic surgical instruments to enable the colonoscopy intervention [7]. Although the robotic capsule endoscopies are more flexible in movement, as the visual field is changing with their orientation, it is not easy to drive the robotic capsule endoscope to a suitable position for intervention. In addition, most operations still need to be controlled manually. In the development of robotic capsule endoscopes, more advanced and automated technologies are required for better assisting physicians in performing difficult procedures during colonoscopy, and for reducing the patient's discomfort.

In this paper, an autonomous colonoscopy intervention is studied on a Robotic Endoscope Platform (REP) [23], with a focus on autonomously delivering the endoscopic surgical instruments to a target polyp. The system is composed of the REP, a user interface, and an auto-feeding mechanism for biopsy instruments. A magnetically tracked sensor was used for acquiring the locations and orientations of REP in real-time. The experimental results of autonomous colonoscopy intervention demonstrate that this system can localize the target polyp and drive the instrument to the polyp position autonomously, all within 60 seconds. This research on autonomous colonoscopy intervention techniques is of great significance in the further advancement of robotic capsule endoscopy solutions.

II. Autonomous Colonoscopy Intervention System Overview

The system for autonomous colonoscopy intervention is shown in Fig. 1. This system consists of the REP, an auto-feeding mechanism, biopsy forceps, and a user interface built in MATLAB. In the colonoscopy, the REP enters the gastrointestinal (GI) tract to inspect diseased polyps, then extends the biopsy forceps and adjusts the device's orientation to treat the polyp.

The REP shown in Fig. 2 (a), is designed to be twice the size (length, height, width) of a previous robotic capsule endoscope as described in [23] for testing in a 2x simulated environment,

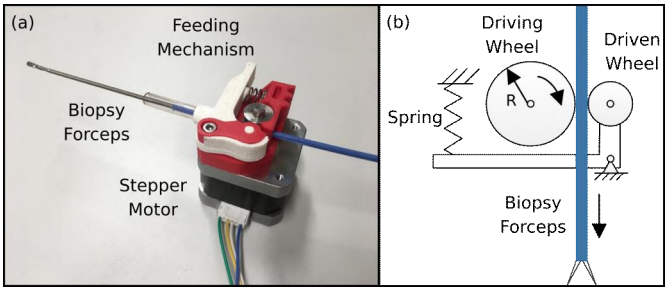

Fig. 3. Auto-feeding mechanism for biopsy forceps. (a) The photograph of auto-feeding mechanism with biopsy forceps; (b) the schematic diagram of the feeding mechanism.

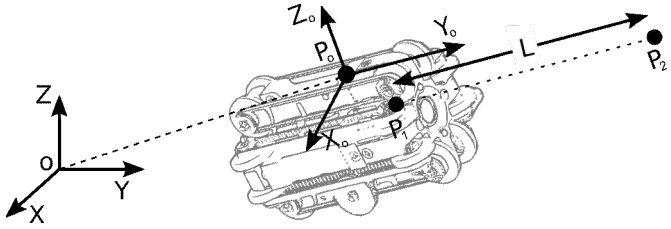

Fig. 4. Workspace analysis of REP. X-Y-Z is the world coordinate system, X_0-Y_0-Z_0 is the REP coordinate system, P_0 is the origin of REP coordinate system and the measuring point of the magnetic sensor, P_1 is the section center of the biopsy forceps at the front end of the REP, P_2 is the end of biopsy forceps, L is the extended length of biopsy forceps.

with a maximum size of 66 x 66 x 105 mm. The REP system is useful for quickly developing and testing strategies for improving GI inspection and surgical treatment. The fully assembled REP consists of four DC motors with encoders, each driving a quadrant of wheels to allow for 2 DOF steering of the device even when rolled over. The top wheels and belts of REP are not shown in Fig. 2 as they were not used in this work. On the front of the REP, two 3 mm LEDs and a monocular camera (ARRIS FPV HD Ultralight CCD Camera, Arris Hobby, ChengDu, China) are installed for real-time visual feedback. A Wi-Fi enabled microcontroller (Photon, Particle Inc., San Francisco, CA) controls the four motors and LEDs. Some autonomous navigation and localization have already been successfully developed on this platform [24], validating the maneuverability and sensing capabilities of this device for implementing control techniques for robotic endoscope applications.

To improve the accuracy and automation of the whole system, the biopsy forceps are extended automatically by the auto-feeding mechanism, as Fig. 1 (d) shows. The auto-feeding mechanism used by the REP can transfer the biopsy forceps forward, while the displacement and velocity are controlled by a stepper motor. As Fig. 3 shows, the auto-feeding mechanism is composed of a driving wheel, a driven wheel, and a tensioning spring. The driving wheel is actuated by the stepper motor, while the driven wheel is forced against the biopsy forceps by the spring so that the forceps can move forward with the rotation of the driving wheel. The spring exerts pressure on the link that connects the driven wheel and with this mechanism, the auto-feeding mechanism can adapt to endoscopy instruments of varying sizes. For the biopsy forceps used in this paper, there is no noticeable slippage during transmission, thus the displacement of the endoscopy instrument can be calculated as $l = 2n\pi R$, in which R is the radius of the driving wheel, and n is the number of motor revolutions.

The work platform in Fig. 1 (c) shows all the devices outside the patient, including the laptop user interface and the auto-feeding mechanism. The user interface sends control commands to the REP and the auto-feeding mechanism. The DC motor control commands for setting wheel direction/speed for the REP are sent wirelessly, while the stepper motor control commands for the auto-feeding mechanism are sent by USB serial connection. A magnetic tracking sensor (Micro Sensor 1.8, Polhemus) is attached to REP to measure its 6 degrees of freedom pose including global position (X, Y, Z) and orientation (pitch, roll, yaw). This pose data is also sent to the user interface. There is a long flexible tube between the auto-feeding mechanism and the REP for transferring the biopsy forceps. As both the tube and the wires for signal transmission are compliant and flexible, the work platform can be moved without hindrance from its attachments.

It is important to note that tools such as the forceps used in this work will not always be needed onboard, but rather are only inserted when some intervention is necessary. In addition, in this paper, biopsy forceps are used as an example of the standard surgical tools. Since the diameters of different surgical tools are similar, the system and method proposed in this paper are applicable to other commercial endoscopic surgical instruments used in traditional colonoscopy.

III. Workspace Modeling of Robotic Endoscope Platform

A. Workspace Analysis of REP with Biopsy Forceps

In colonoscopy intervention, it is important to know the real-time end position of the biopsy forceps, such that it can successfully extend to the polyp. The collection of all possible end positions of the biopsy forceps represents the reachable workspace of this system and depends on both the pose of the REP and the extension length of the biopsy forceps. Therefore, the modeling of the workspace for predicting the end position of the biopsy forceps is shown here.

To describe the end position of biopsy forceps, a world coordinate system is defined as the center of the magnetic source of the magnetic tracking system. As shown in Fig. 4, X-Y-Z defines the world coordinate system, and X_0-Y_0-Z_0 is used to describe the local REP coordinate system. P_0 is the measuring point of the magnetic sensor which is used to measure the pose of the REP, and is also the origin of the REP coordinate system. P_1 is the section center of the biopsy forceps at the front end of the REP, and P_2 is the end of biopsy forceps. L is the extended length of biopsy forceps from the front of the REP and along the direction of Y_0 in the REP coordinate system. For simplification, the initial REP coordinate system is parallel to the world coordinate system, in which X, Y, Z axes have the same directions as that of X_0, Y_0, Z_0 axis. This is

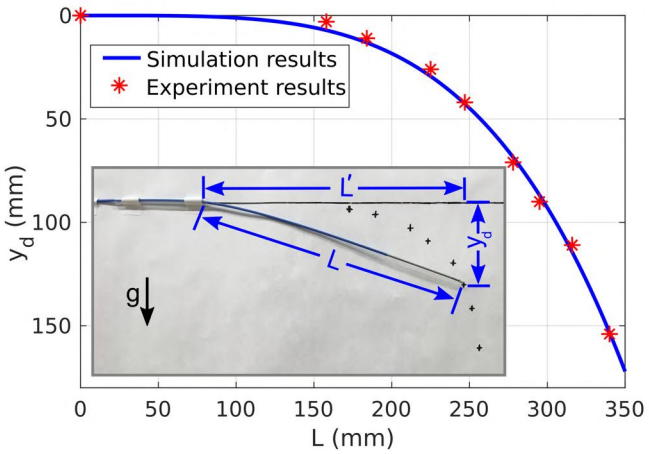

Fig. 5. Comparison of the experiment results and the simulation results of biopsy forceps deflection.

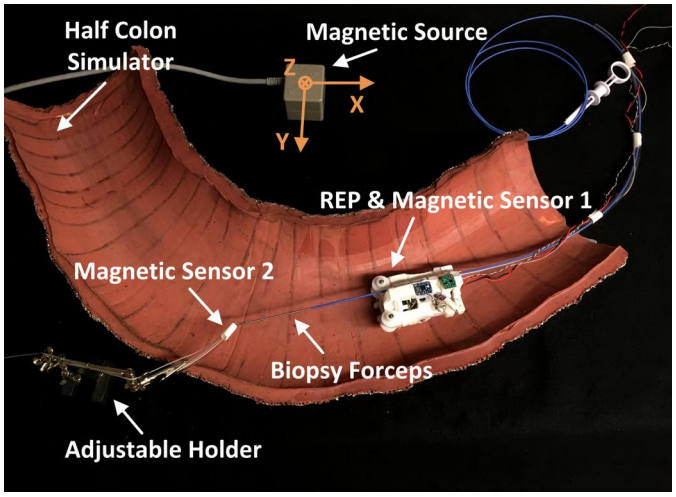

Fig. 6. Experiment setup for verifying the workspace model of REP.

achieved by adjusting the initial pose of the REP to make the two coordinate systems parallel, and then then zeroing out the orientation of the sensor. In this case, the pose of the REP can be calculated by its movement transformation matrix. According to the orientations of the REP coordinate system, P_2 in the world coordinate system can be calculated by (1).

$$P_2 = R_{\psi,Z}R_{\theta,Y}R_{\varphi,X}(P_1^0 + [0 \quad L \quad 0]^T) + P_0 \tag{1}$$

In which ψ, θ, φ are the Euler angles of REP coordinate frame with respect to world coordinate frame, $R_{\psi,Z}$, $R_{\theta,Y}$, $R_{\varphi,X}$ are the corresponding rotation matrices. P_1^0 is the position vector of P_1 relative to P_0 in the REP coordinate system.

In (1), the extension of biopsy forceps is considered as a straight line that is parallel to the REP with a length of L. However, due to its own weight, a gradually increasing deflection occurs with the extension of the biopsy forceps. Therefore, the deflection must be considered in the workspace model. As the deflection phenomenon is similar to cantilever beam deflection, a formula similar to the cantilever beam deflection model is used to fit the deflection of the biopsy forceps. The relationship between the deflection and extension length of biopsy forceps is then modeled as (2).

$$y_d = 1.147\times10^{-8}L^4(mm) \tag{2}$$

The comparison of experimental results and model simulated results of biopsy forceps deflection is shown in Fig. 5, the gravity direction is vertically downward. The model shows a good match to the measured deflection, with an R-square value of 0.9973, and an RMSE of 2.6 mm. The L' in Fig. 5 can be approximately calculated by (3).

$$L' = (L^2 - {y_d}^2)^{1/2} \tag{3}$$

Substituting (3) and (2) into (1), the end position of biopsy forceps P_2 can be calculated by (4).

$$P_2 = R_{\psi,Z}R_{\theta,Y}R_{\varphi,X}(R_{-\theta,Y}[0 \quad L' \quad y_d]^T + P_1^0) + P_0 \tag{4}$$

Note that the forceps' deflection is generated in the direction of gravity. When the REP rotates along the Y_0 axis at an angle of θ, the bending forceps is no longer parallel to the X_0Y_0-plane. In this condition the coordinates of the biopsy forceps' end can be calculated as $R_{-\theta,Y}$* $[0, L', y_d]$.

B. Experiment for Evaluating Workspace Model

The workspace model presented in (4) was evaluated by the experimental platform shown in Fig. 6. The REP was placed on the half colon simulator which is a synthetic super-soft silicone colon halfpipe (Ecoflex® Series 00-10, Smooth-On Inc., Macungie, PA), similar to that used previously in the actuated colon simulator [25]. As noted previously, the world coordinate system is defined by the magnetic source of the sensor tracking system and the pose of the REP is measured within this world coordinate frame by a magnetic sensor, with a second sensor used to measure the end position of the biopsy forceps as ground truth. As the sensor is magnetically tracked, it is sensitive to external magnetic fields, including those induced by ferrous metal. To avoid inducing additional error in sensor measurements caused by the metal gripper of the biopsy forceps, the second sensor was mounted via a plastic tube with an adjustable holder. With the adjustable holder, the sensor can be placed close to the end position of the biopsy forceps, such that the pose of this tool can be accurately measured within the world coordinate system. In this experiment, the REP was placed in multiple positions with different orientations, and with various extension lengths of the biopsy forceps in each position. The sensor data were recorded in each trial, and the end positions of the biopsy forceps were calculated by the workspace model. The comparison of experimental results and simulation results of the end positions of the biopsy forceps are shown in Fig. 7.

Fig. 7 (a) shows the experimental results and simulation results of the end position of the biopsy forceps in 3D space, with Fig. 7 (b) showing the absolute errors. In Fig. 7 (b), the points with the same extension of biopsy forceps were collected in different poses of the REP, and the points with different extension of biopsy forceps came from a constant REP's pose. It is clear that the absolute errors are all under 0.7 cm. If we define the relative error as the ratio of absolute error to the

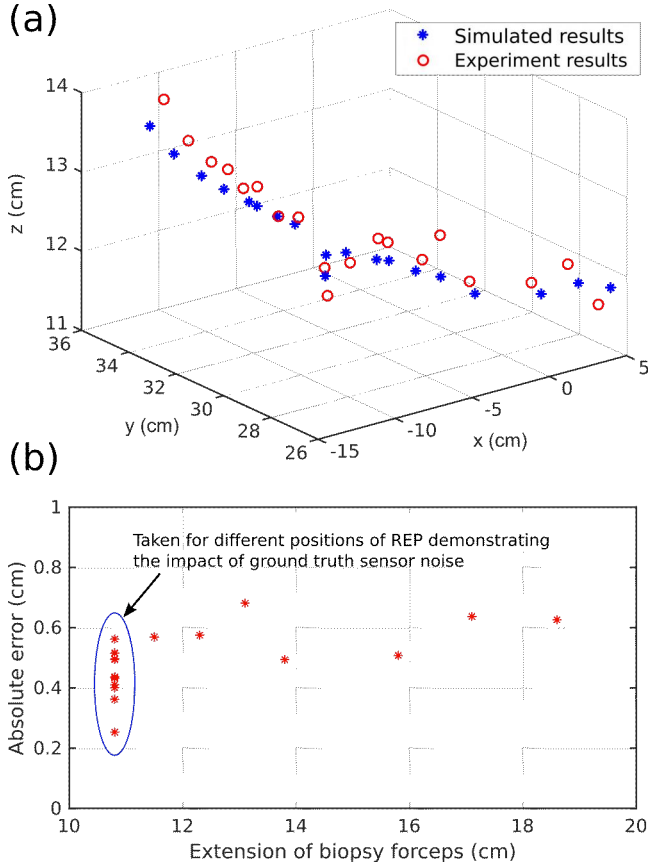

Fig. 7. Comparison of experimental results and simulation results of end position of biopsy forceps. (a) Comparison of experimental results and simulation results in 3D space, (b) relative error analysis. The relative error is the ratio of absolute error to the extension length of biopsy forceps. Note that while the extension of the forceps appears to have little impact on accuracy, absolute accuracy can improve when the REP is situated close to the magnetic source and with no sources of magnetic interference in the vicinity as indicated by the noise seen from the first position of the biopsy forceps.

extension length of biopsy forceps, the relative errors are all below 5.5%. It can be seen that the experimental results are in good agreement with the simulated results. The two primary sources of error are responsible for this discrepancy including the model error, inherent to the simplified deflection model of the biopsy forceps, as well as the measurement error of the sensor. This measurement error is significant and cannot be ignored, as the system itself has an error range of at least 1.5 mm in position and 0.4° in orientation according to the manufacturer. Moreover, the magnetic interference with the pipe of the colon and the biopsy forceps also cause the sensor measurement error. According to Fig. 7 (b), a small error fluctuation is observed when the REP posture is unchanged, while the error varies greatly along with the changed REP's pose. This demonstrates that the primary source of error is the magnetic sensor itself, while the deflection model generally maintains high accuracy throughout.

IV. Position Estimation of Target Polyp

A. Position Model of Target Polyp

As the biopsy forceps can only extend and retract, during colonoscopy intervention the REP is required to move to a position with suitable posture such that the biopsy forceps can be extended to reach the target polyp. Using the workspace model, the real-time end position of the biopsy forceps can be predicted. To determine whether the biopsy forceps can reach the target tissue in its current posture, it is necessary to know the position of the target polyp. An image based estimation of the polyp position is thus carried out.

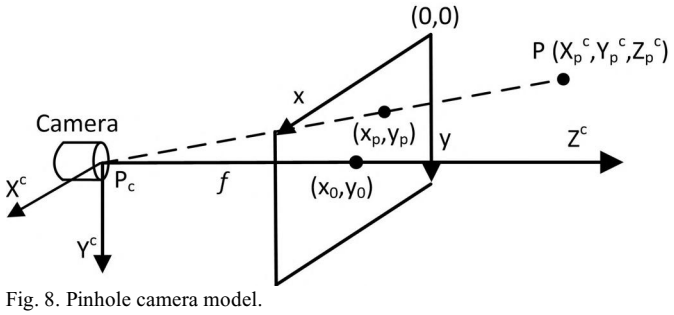

Fig. 8. Pinhole camera model.

Fig. 8 shows a pinhole camera model, where X^c-Y^c-Z^c is the camera coordinate system, the image plane x-y is the camera projection plane. P_c is the origin of the camera coordinate system, the physical distance between P_c and the image plane is the focal length f. P is a random point in 3D space, $(x_p,\ y_p)$ is the projection of P on the image plane that expressed as pixel coordinates, and $(x_0,\ y_0)$ is the pixel coordinates of the camera center in the image plane. The coordinates of P in the camera coordinate system can be calculated by the following equation.

$$\begin{bmatrix} X_p^c \\ Y_p^c \\ Z_p^c \end{bmatrix} = Z_p^c \begin{bmatrix} (x_p - x_0)/f \\ (y_p - y_0)/f \\ 1 \end{bmatrix} \tag{5}$$

Considering the coordinate system transformation from the camera coordinate system to the world coordinate system shown in Fig. 4, the coordinates of point P in world coordinate system can be expressed as (6), in which $[X_p^c \quad Z_p^c \quad -Y_p^c]^T$ is the rotated coordinates of point P from the camera coordinate system to REP coordinate system.

$$\begin{bmatrix} X_p \\ Y_p \\ Z_p \end{bmatrix} = R_{\psi,Z} R_{\theta,Y} R_{\varphi,X} \left(\begin{bmatrix} X_p^c \\ Z_p^c \\ -Y_p^c \end{bmatrix} + P_c^0 \right) + P_0 \tag{6}$$

Here, P_c^0 is the position vector of P_c relative to P_0 in the initial REP pose in the world coordinate system.

As there is only a single camera on the REP, it cannot obtain the absolute depth of the target point P, which refers to Z_p^c in (6). In this condition, for a single set of the measured data including magnetic sensor measurement data and the pixel coordinates of the target point in a recorded image, it only provides an estimated straight line that passes through P and P_c. Theoretically, to determine the coordinates of the target point, at least two such estimated lines are needed such that their point of intersection can be determined. However, in practical applications, the two estimated lines are unlikely to intersect in 3D space due to measurement errors, therefore an optimal

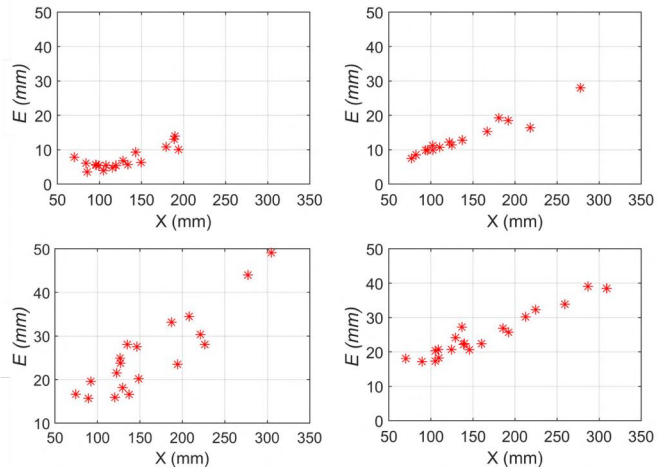

Fig. 9. Accuracy analysis of the collected data for estimating the polyp position. *X* is the distance between the REP and target polyp, and *E* is the distance between the target polyp and the estimated line.

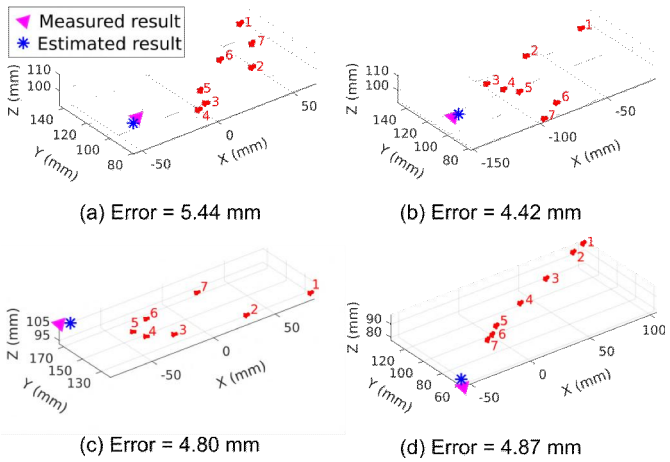

Fig. 10. Comparison of measured ground truth result and estimated result of the four polyp positions. Purple triangle is the measured ground truth polyp position, blue star is the estimated polyp position, and the red markers are the camera poses for each view.

position of the target point is calculated instead [26]. To further improve the estimation accuracy, multiple views are used for estimating the position of the target point.

B. Verification Experiment of the Position Model

To verify the position model and the proposed method for estimating the coordinates of the target polyp, a platform similar to the platform in Fig. 6 is used, where one magnetic sensor was attached to the REP to measure its pose, while a second sensor was used to measure the position of the polyp. The polyp used in this initial experiment is also made by synthetic super-soft silicone (Ecoflex® Series 00-10, Smooth-On Inc., Macungie, PA), and has a diameter of 2 cm. This polyp can be seen in Fig. 2. The pose data and the images taken by the REP's camera were collected in this experiment.

To improve the accuracy of this estimation technique and to find the effective distance of the REP for detecting polyps, the accuracy of the collected data for predicting the target point is assessed in a simple experiment performed on the platform. In this experiment, 20 views along with ground-truth REP poses were collected as the REP views the 2 cm polyp and with the polyp in four different positions within the simulated environment. In each view, the pixel coordinates of the polyp position are measured. According to (6), an estimated line that passes through the camera center and the target polyp can be calculated. For a perfect estimation on the target polyp, the target polyp should be on the estimated line, as the greater the deviation between the polyp and the estimated line, the lower the estimation accuracy. The distance between the target polyp and the estimated line and the distance between the REP and the target polyp are observed in Fig. 9. The *X* is the distance between REP and target polyp, and the error, *E* is the distance between the target polyp and the estimated line. In general, *E* increases with the growth of *X*. To reduce the error generated by the remote measurement distance, it is better to use the data with a shorter measurement distance (under 200 mm). Therefore, the experimental assessment of polyp position estimation is carried out within a measurement distance of 200 mm.

In this experiment for estimating the polyp position, the REP maneuvers on the half synthetic colon to observe the polyp, and multiple views (7 views) were recorded for estimating a fixed polyp position in each experiment. Four sets of experiments with different polyp positions were tested in total (Fig. 10). In the experiment, the tracking area on the polyp was manually selected with the measured position of sensor 2 serving as the center of the tracking area. All of the feature points within this area were then reconstructed by the position model of the polyp. The average value or centroid of these points was then calculated to define the estimated polyp position.

The estimated positions and the measured ground truth positions of the four polyp positions are presented in Fig. 10. The blue star is the estimated polyp position while the purple triangle is the measured ground truth polyp position. The red markers are the camera poses for each view. The error is the distance between the estimated position and the measured position. These absolute errors of the four experiments are all less than 5.5 mm. This error may be due to several aspects of this experiment including limitations on camera intrinsic calibration accuracy as well as the resolution limitations of the magnetic sensors which can substantially impact the measurement accuracy of the polyp and the REP position and orientation. In general, the accuracy of this method is still more than sufficient as most polyps that need colonoscopic intervention are larger than 6 mm [27].

V. Autonomous Control of Colonoscopy Intervention

With the workspace model and position model for the polyp validated, we are now able to estimate the two critical positions of the biopsy forceps end and the polyp. On this basis, we can carry out the autonomous colonoscopy intervention as follows. First, when the REP drives near a suspected polyp (as observed via real-time camera feedback), the REP is manually stopped to provide a good view of the polyp. The user then manually selects the tracking area on the

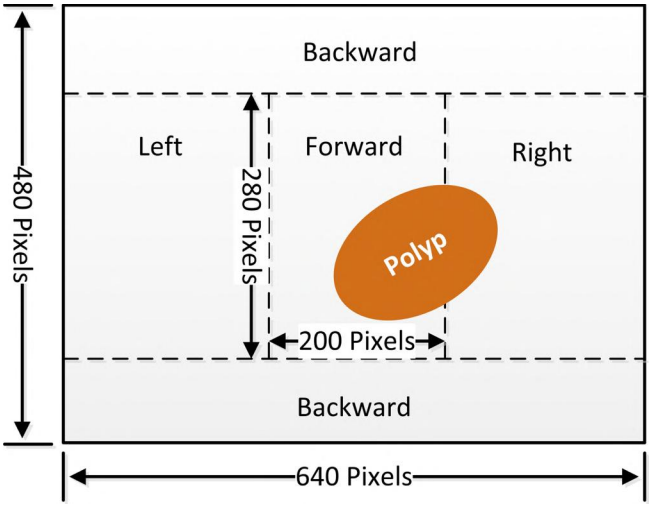

Fig. 11. Autonomous driving strategy of REP for tracking polyp and recording multiple views. The descending priority of the four commands are Backward, Left, Right, and Forward.

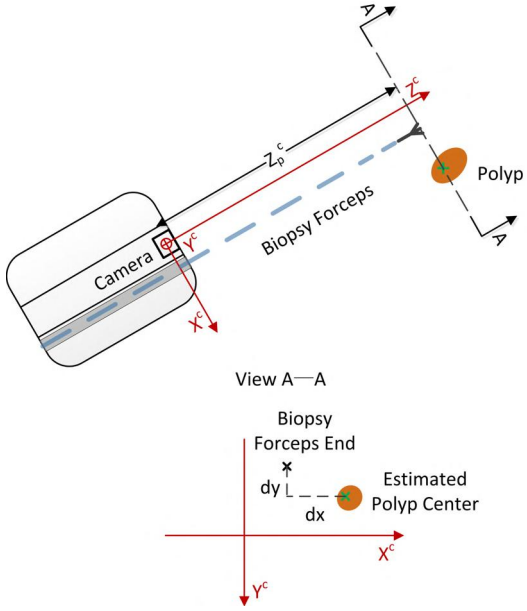

Fig. 12. Autonomous pose adjustment of REP. In this method, by controlling the REP motion to reduce the position difference dx and dy, the end of the extended biopsy forceps will close to the target polyp.

suspected polyp for colonoscopy intervention by tracing a bounding box around the polyp within the MATLAB interface. This is the only step in the autonomous colonoscopy intervention that requires manual operation by the physician who must decide which areas or polyps require interventions. The remainder of the process is automatically completed by the robotic system. Once the polyp area has been selected, the REP will automatically take several views of the selected area in different positions and orientations. Once these images have been captured the system will estimate the position of the centroid of this area from both the captured views and the measured REP pose data using the method presented in Section Ⅳ. According to the estimated polyp position, the REP will autonomously adjust its pose to extend the biopsy forceps for colonoscopy intervention. This process includes two autonomous driving procedures. The first one is to take different views of the polyp for reconstructing its 3D position

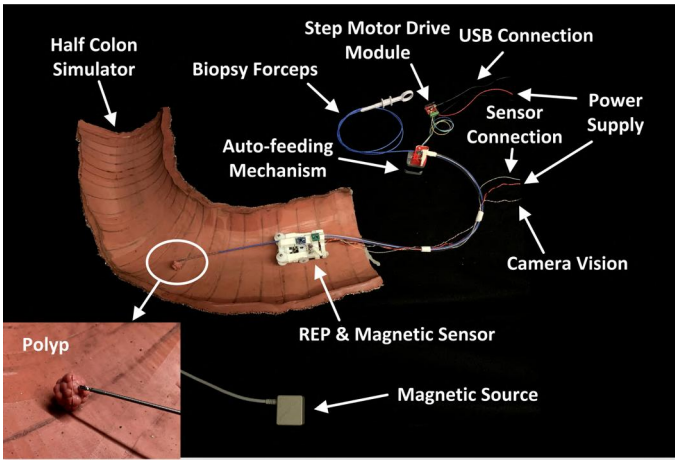

Fig. 13. The autonomous colonoscopy intervention experimental setup.

in the world coordinate system. The second procedure adjusts the REP's location and orientation such that the extended biopsy forceps can reach the target polyp.

The autonomous driving strategy of the REP for recording multiple views of the polyp is shown in Fig. 11. The size of a single view is 640x480 (pixels), and each view is divided into 5 regions, where the size of the central region is 200x280 pixels. The regions in the top and bottom are Backward regions, the left and right regions are defined as Left and Right regions respectively, and the central region is the Forward region. The name of each region corresponds to the command of the REP motion, and the priority of the four commands follows a descending order of Backward, Left, Right, and Forward. For example, as Fig. 11 shows, the polyp occupies two regions (Forward and Right), as the Right command has priority over the Forward command, the REP will first receive a Right command and begin turning right followed by the Forward command for the next motion. In the first frame of view, the polyp should be fully present. This is applicable in practice because we can stop the REP when we fully observe the polyp, then select the tracking area via a bounding box on the polyp in the first view. The REP will follow these commands to continue moving and tracking the polyp, and will then extract 7 views (at equal time intervals), from the recorded views. Of these commands, the Backwards is the highest priority commands because it will capture a larger range of the scene; under this circumstance, the tracking loss can be significantly avoided. What's more, if the backward region is relatively narrow, the polyp will be easily seen in the middle regions so that the REP is less likely to travel far from the polyp. In this case, the estimation error on the polyp position caused by the significant distance between the REP and the polyp can be largely avoided. The Forward region is relatively small because the REP is encouraged to take views in different orientations to provide a larger baseline between views and thus a more accurately estimated 3D location of the polyp. There is no fixed order for the priority of Left and Right commands, which means the priority order of the two commands can be reversed.

The second mode of autonomous driving for the REP is an adjustment to its location and orientation according to the estimated polyp position. The control strategy for autonomous

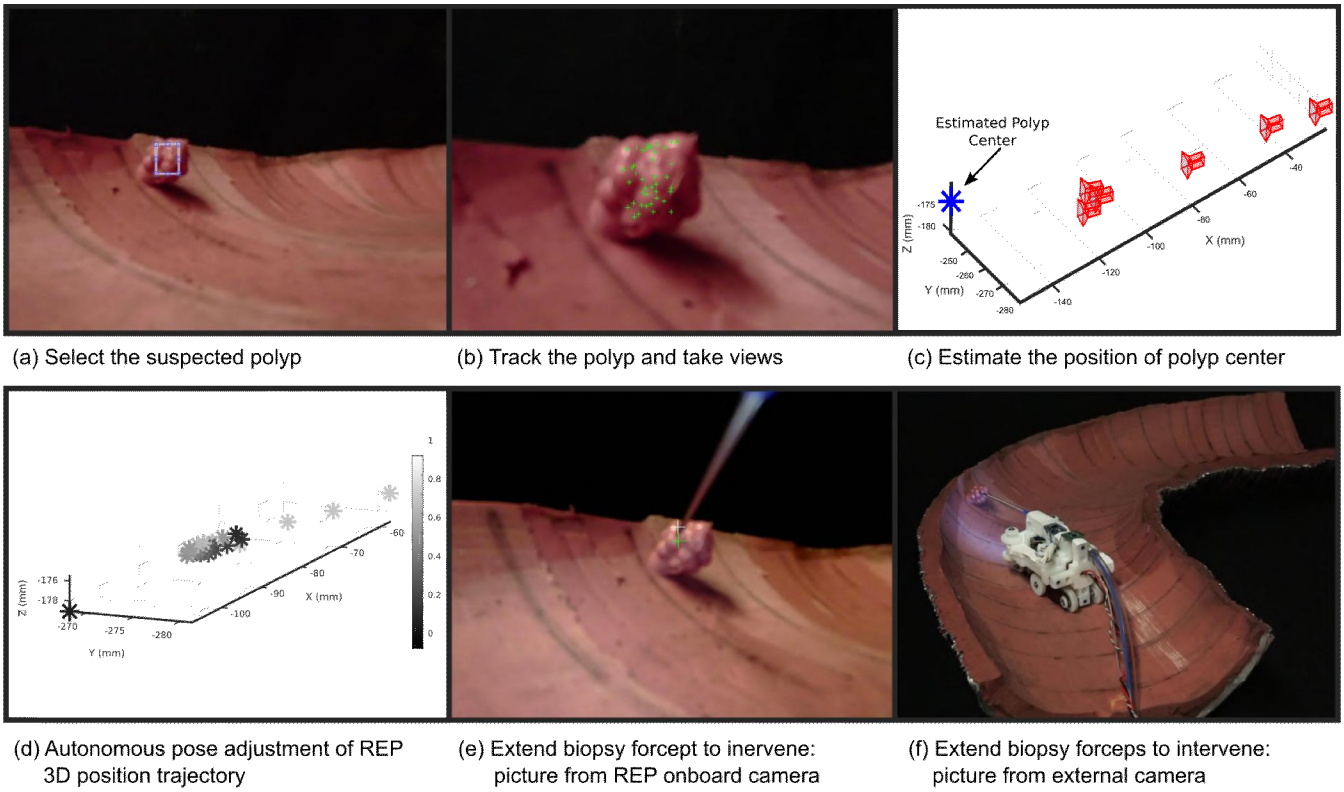

Fig. 14. Experimental results of the colonoscopy intervention. (a) select the suspected polyp, (b) track the polyp and take multiple views, (c) estimate the position of polyp center. (d) autonomous pose adjustment of the REP: 3D position trajectory, (e) extend biopsy forceps to intervene: picture from the built-in camera, (f) extend biopsy forceps to intervene: picture from the external camera.

pose adjustment is explained in Fig. 12. The camera and biopsy forceps have the same orientation as that of REP, and thus for simplicity, we consider them within the camera coordinate system. In Fig. 12, the Z^c-axis coordinate of the estimated polyp in the camera coordinate system is Z_p^c. The coordinates of the end of biopsy forceps with a Z^c -axis coordinate of Z_p^c can be estimated by the workspace model. View A-A is the view plane that contains the estimated polyp position and is perpendicular to the Z^c axis. As View A-A shows, the black x-marker is the end position of biopsy forceps, the green x-marker is the estimated polyp position. dx and dy are the position differences between the two crosses in X^c axis and Y^c axis respectively, which are defined as the difference between the biopsy forceps end and polyp center.

To adjust its pose for colonoscopy intervention, the REP will turn left or right to reduce the absolute value of dx within an error tolerance x_{err}. The REP will then move forward or backward to reduce the absolute value of dy to within an error tolerance y_{err}. The haustral folds in the colon lumen can affect the pitch angle of the REP, as a result, the Y^c coordinate of the end of biopsy forceps can be changed. However, it is difficult to control this unknown environmental factor, therefore we make use of the deflection of the biopsy forceps to adjust the end position of these forceps in the Y^c direction instead. If $dy > 0$, which indicates the end of the biopsy forceps is higher than the polyp center, the REP will move backward and Z_p^c will increases such that the deflection of the biopsy forceps will increase to reduce the absolute value of dy. In contrast, if $dy < 0$, the REP will move forward to reduce the deflection of the biopsy forceps thereby reducing the absolute value of dy. Once both dx and dy are within the error tolerances, the REP will stop, and the current posture of REP is considered to be a suitable posture for colonoscopy intervention. The auto-feeding mechanism will next transmit the biopsy forceps to the position of the polyp. When the end of the biopsy forceps is placed at the inlet of the long tube connected to the auto-feeding mechanism, the feeding length of biopsy forceps is the sum of the tube's length and extension of the biopsy forceps, in which the extended length of biopsy forceps can be calculated according to (2) with the known deflection.

VI. Experiment of Autonomous Colonoscopy Intervention

A. Experiment Process and Results

To evaluate the performance of this autonomous colonoscopy intervention method, the following experiment was carried out and the process and results are shown. Fig. 13 presents the experiment platform, with the REP on the half colon simulator. A magnetic sensor was affixed to the REP to measure its locations and orientations. The motor drive module is used for driving the stepper motor of the auto-feeding mechanism, and it receives control commands from the user interface via the USB connection. Views from the onboard camera were sent to the user interface by a USB cable.

The experimental process and the results of the autonomous colonoscopy intervention are shown in Fig. 14. First, the

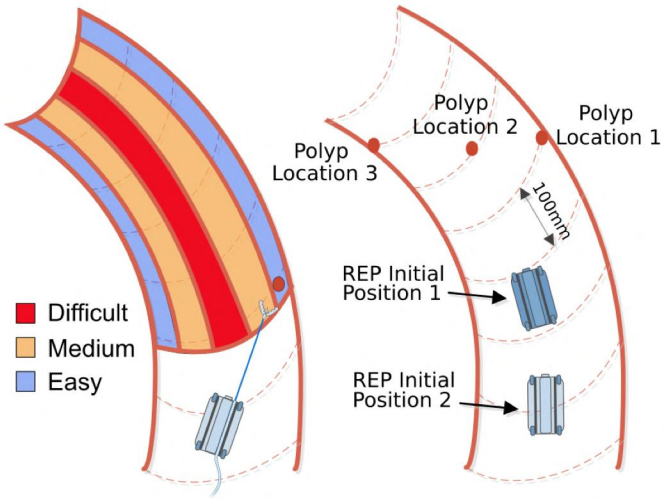

Fig. 15. The autonomous colonoscopy intervention experiments. Level of difficulty is somewhat determined by the polyp position. Polyps lower in the workspace require a longer extension of the forceps to allow for greater deflection (left), this results in a greater challenge for the REP. Note that polyps above the plane of the surgical tool can be accessed by reducing the insufflation pressure within the colon and allowing the tissue to partially collapse. For this experiment (right), the polyp is placed in three locations, i.e., the right side, the middle bottom, and the left side of the colon simulator; the REP has two initial positions for each target polyp position, in which the two initial positions are 100 mm and 250 mm away from the target polyp location in the direction of the center line.

tracking area on the target polyp was manually selected on the inspection screen of the user interface, as Fig. 14 (a) shows. The REP can then track the features of this selected area, as Fig. 14 (b) shows, with five views along with the REP pose data as measured by the magnetic sensor and collected during this period. With this data and the polyp position model, the selected area can be reconstructed. Removing some of reconstruction points outside the valid region with a simple polyp location estimation, in which the valid region of the polyp position is estimated as within 200 mm of the forefront of the REP polyp tracking route. Then the average value of the remaining points serves as the final estimated polyp position. The estimation of the polyp position and the camera pose corresponding to the five views are shown in Fig. 14 (c). Using the autonomous pose adjustment strategy, the REP can move itself to a position that satisfies the colonoscopy intervention requirement. In this experiment, the tolerance x_{err} and y_{err} are set as 3 mm and 5 mm respectively. The trajectory of REP pose adjustment recorded by the magnetic sensor was presented in Fig. 14 (d), it can be seen that about 15 seconds was spent in total, with the orientation adjustment carried out first and requiring the most time in this process. Fig. 14 (e) and (f) show the results of extending the biopsy forceps to the polyp in this experiment; Fig. 14 (e) was taken from the built-in camera on the REP, while the Fig. 14 (f) was observed by the external camera. In Fig. 14 (e), the green cross is the estimated center of the selected area, while the white crossing marker is the real-time estimated end position of biopsy forceps when it is extended to the polyp position. It can be seen that the tip of the extended biopsy forceps is located on the position where the white cross is marked, and the green cross is near the center of the selected area. According to the location of the two crosses, it can be concluded that the workspace model has high accuracy and the polyp position model and optimization method also work well in predicting polyp position. The entire experiment took approximately 1 minute, including the selection and tracking of the polyp, the position estimation of the polyp, the pose adjustment of the REP, and extension of the biopsy forceps to the polyp position. Thus it is clear that the REP can successfully perform an autonomous colonoscopy intervention in this simulated environment using the method described here.

TABLE I
SUCCESS RATE OF AUTONOMOUS COLONOSCOPY INTERVENTION[1]

Polyp Location	REP Initial Position	Polyp size		
		1 cm	2 cm	3 cm
Location 1	Position 1	43%	57%	71%
	Position 2	43%	71%	71%
Location 2	Position 1	43%	57%	100%
	Position 2	14%	71%	71%
Location 3	Position 1	57%	86%	100%
	Position 2	57%	57%	71%
Mean Success, All Trials		43%	67%	81%

[1] success rate is calculated as the mean of 7 trials for each polyp position and REP initial position.

B. Experiment Dataset of Autonomous Colonoscopy Intervention in a Smooth Half-Pipe Simulator

To evaluate the repeatability and success rate of the proposed autonomous colonoscopy intervention method, a series of experiments with different polyp sizes, polyp locations, and initial positions of REP is performed. Three polyps with different diameters are tested, i.e., 1 cm, 2 cm, and 3 cm, each polyp is placed in three different locations in the colon simulator. As Fig. 15 shows, the distance between two adjacent polyp locations in the direction of the centerline of the colon simulator is 100 mm. The colon simulator is on a horizontal table, polyp locations 1 and 3 are on the left and right sides of the colon simulator (effectively at the centerline height of the colon), while the polyp location 2 is on the bottom and is 50 mm lower than locations 1 and 3 in height. In polyp locations 1 and 3, a small deflection with a short extension of biopsy forceps will allow the biopsy forceps to touch the target polyp, however a large deflection along with a long extension of the biopsy forceps is needed for a lower polyp position in Location 3. For each polyp position, the REP will start from two initial positions, and each position will perform 7 trials. As Fig. 15 shows, the REP initial position 1 is 100 mm away from the target polyp in the direction of the center line and position 2 is 250 mm. For polyp locations 1 and 2, the REP is located in the middle of the colon simulator and parallel to the colon's centerline in both initial positions. For polyp location 3, the two initial REP positions have an orientation of 45 ° left along the centerline of the colon simulator to make the polyp insight. It should be noted that while no testing was done on polyps above the height of the surgical tool within the half-pipe environment, in practice, decreasing the insufflation pressure within the colon easily allows for the target polyps to be lowered and maintained at a position within the REP workspace, and thus these targets can be placed at the height that is most easily reached by the tool (polyp location 1).

In the experiments, a successful result is defined as the end forceps touching the polyp. The experimental results for each experiment setup are shown in Table I, with the number of successes in every seven trials. For example, there are three successful trials in the seven trials with polyp size of 1 cm, polyp location 1, and REP initial position 1. It is reasonable that

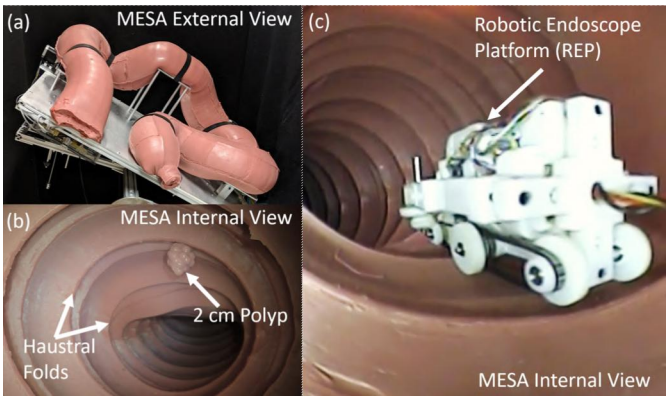

Fig. 16. A full external view of the MESA simulation environment is shown (a) as well as an internal view and 2 cm polyp present (b). The REP is shown inside of the fully insufflated MESA in (c).

the success rate is higher when the polyp size is larger, and the general success rate is better when the REP starts in position 1 which is closer to the target polyp. Larger polyps have more reachable areas and therefore more tolerance for the intervention, while the closer initial position of REP will allow better extraction and tracking of polyp features due to the larger occupied area of polyp in the initial image. It can be seen that there is only one success in the seven trials with the 1 cm polyp, polyp at location 2, and the REP in initial position 2. In this experimental setup, the polyp is too small to extract features at such a long-distance view and the biopsy forceps must also extend a long distance to generate a large deflection and thus reach the small polyp, since the polyp is too small, a small positional deviation will cause the biopsy forceps to deviate from the polyp, the average deviation from the polyp surface is 1.3 cm in this experiment. In general, the success rate of autonomous colonoscopy intervention is approximately 43% with the 1 cm polyp, 67% with the 2 cm polyp, and 81% with the 3 cm polyp.

C. Experiment Results of Autonomous Colonoscopy Intervention in a Closed Colon Simulator

To test the performance of the autonomous colonoscopy intervention in a closed colon environment, two closed colon simulators were used. As Fig. 17 (a) shows, the first closed colon simulator is composed of the original simulator used for the above experiments, with its symmetric top half added. This allows for a more realistic environment with no external illumination. The second colon simulator shown in Fig. 16 and Fig. 17 (b) is the Modular Endoscopy Simulation Apparatus (MESA) [25]. This simulated environment consists of a molded silicone colon and also includes realistic haustral folds on the inner walls which serve as obstacles to the REP. As evaluated in [24], the MESA environment demonstrates excellent visual accuracy to that of the actual colon, while also being extremely soft and deformable and capable of complete internal collapse if insufflation is reduced. While both of these environments are more realistic and serve as important testbeds for validating the previous results, their closed, inaccessible nature is not ideal for repeatable testing and ground truth validation, and thus, why they were not used in the initial experimental work seen above.

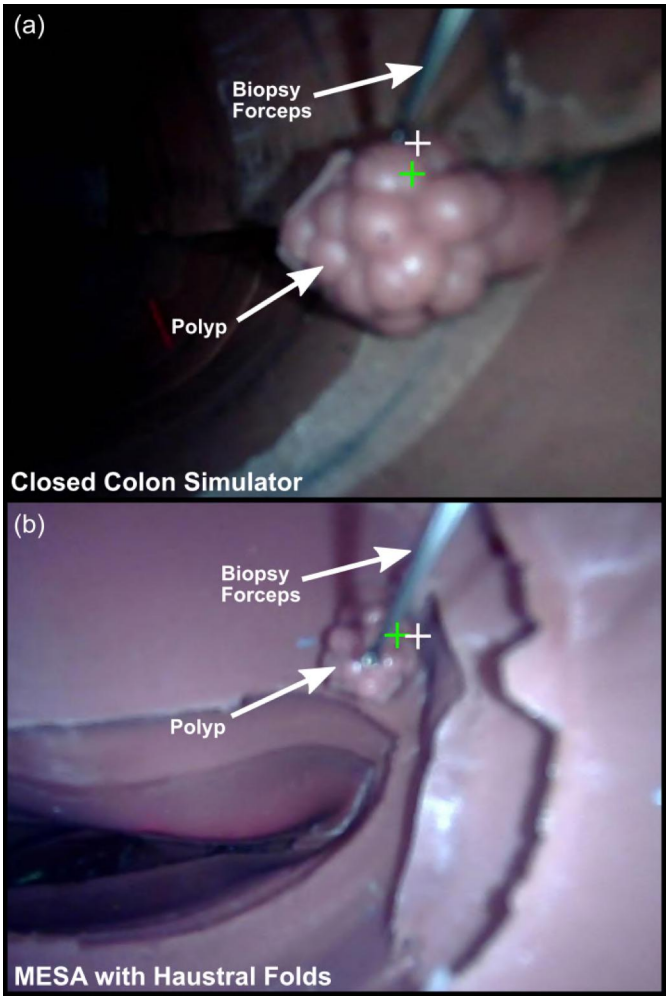

Fig. 17. The autonomous colonoscopy intervention experiments in the closed colon environment, the biopsy forceps reached to the polyp in both of the two closed colon simulators. (a) the closed colon simulator is composed of the two half colon simulators, and has a dark inside environment; (b) the Modular Endoscopy Simulation Apparatus (MESA) has haustral folds which are similar to that in the biological colon, and serve as obstacles and disturbances during colonoscopy. Note that in this case the target polyp is above the plane of the surgical tool, but the folds allow for the device to pitch upwards slightly to reach this target. In both images, the white marker is the estimated forceps final position, while the green marker is the estimated polyp centroid

Note that in each of the two experiments, lighting is only provided by the REP's onboard LEDs.

The experiments were conducted following the process shown Fig.14, and the biopsy forceps successfully reached the polyp positioned in each of the two closed colon simulator environments. No significant performance differences in autonomous colonoscopy intervention were observed between experiments in the closed colon simulator and the half colon simulator, including the operation time and accuracy. In the case of MESA with haustral folds, the REP did have difficulty with mobility over the haustral folds during the autonomous intervention. The haustral folds slow REP's movements and can result in large vibrations as the REP attempt to align with the target polyp. This vibration makes tracking of features on the polyp more difficult (due to motion blur), and thus affects the estimation accuracy of the polyp position. Moreover, the vibration of the REP can also lead to an unstable posture, such

that more time is required to adjust its posture before the forceps are extended.

According to the two experiments, the dark environment in colon did not significantly impact the performance of this autonomous colonoscopy intervention strategy, while the REP's vibration caused by the haustral folds did create difficulties. To overcome this problem, faster and more robust motion control methods for the REP need to be used in the future. In addition, while the position of the polyp is assumed to be constant in this paper, in actual surgery, it may change slightly due to the patient's breathing and gastrointestinal movements. Therefore, the control method for autonomous colonoscopy intervention should also account for this problem. An additional challenge during the experimental evaluation in the MESA simulator was the fact that the target polyp was placed at a height above the plane of the REP tool. Unlike the smooth environments, the MESA simulator's haustral folds allow for some pitching of the REP during testing. This allows for expansion of the REP workspace and thus intervention even in the case of the target that otherwise would have required deinsufflation to reach.

VII. Results & Discussion

With the proposed control strategy for autonomous colonoscopy intervention, the REP can autonomously adjust its pose and extend the biopsy forceps to the polyp based on the estimated positions of the target polyp and the forceps end. The effectiveness of the proposed control strategy was confirmed by the autonomous colonoscopy intervention experiments on a half colon simulator. In the experiment, the whole process for autonomous colonoscopy intervention takes less than 60 seconds, including the communication setup with the REP controller, tracking and capturing views of the polyp, autonomous pose adjustment of the REP, and all model calculations. The REP only spent 15 seconds on average in finding a suitable location to extend the biopsy forceps for colonoscopy intervention. The success rate of autonomous colonoscopy intervention is more than 43% with a 1 cm polyp, and up to 81% with a 3 cm polyp. Furthermore, the autonomous colonoscopy intervention on the REP is tested in two closed colon simulators, and the biopsy forceps can be successfully extended to the target polyp. This is successful even in the case of a target polyp that is above the plane of the surgical tool within the MESA simulator due to the pitching allowed by the haustral folds that are present within this environment. Similarly, a negative pitching of the REP can allow for reaching a low lying polyp that is close to the REP with a shorter length of surgical tool. This is undoubtedly beneficial for intervention within the limited space of the tortuous colon where visualization and intervention over longer distances may not be desired or even possible.

According to the experiments, the key to the success of this autonomous colonoscopy intervention approach lies in the accuracy of the polyp position estimation. In this paper, the polyp position is only estimated based on the polyp position model and the input of the REP pose and tracked features; no additional measurements are taken to detect the real-time errors and adjust the polyp position estimation during this process. In addition, the control strategy presented here for autonomous colonoscopy intervention is relatively simple with only bang-bang control being utilized for setting REP wheel speed and direction (i.e., the REP is either driving forward, backward, or turning at full speed in response to the polyp positional feedback in each image). While this strategy is successful in our simulated environments, real-time polyp positional error and fine-tuned motor control strategies may be necessary in the more complex and variable in vivo environment or if smaller polyps are to be biopsied with high precision. To improve the accuracy of colonoscopy intervention, higher precision control strategies utilizing updated real-time polyp and tool position estimates will be developed in future studies. We expect that by both carefully controlling the REP pose, and by adding real-time closed-loop control during the intervention process (by accounting for spatial errors between the forceps tip and target polyp) we will be able to substantially improve the accuracy of this method. This can be readily achieved from visual feedback utilizing similar object tracking strategies to those employed in polyp tracking and will serve to further augment this method for autonomous colonoscopy intervention.

For future transition back to scale, it should be noted that while these experiments utilize a 2x scaled system and environment, the transition of this strategy to a 1x system such as that used in [16] should not require substantial changes beyond adjustment to the controller and thresholds used. This is expected because like the scaling of the overall system, the onboard camera used for sensing on this larger system, necessarily requires a much longer focal length (approximately twice that of the Endoculus in [16]). Thus, given the smaller *in vivo* environment coupled with the smaller focal length camera, we would anticipate much shorter intervention distances, less tool deflection and in general, comparable performance to the experiments demonstrated here.

While the results shown here evaluate the critical metrics for proving the utility of autonomous intervention onboard a robotic endoscope, additional concerns such as patient safety must also be considered going forward. Currently this system does not evaluate this critical factor, however visual or force feedback to alert a physician of tool-tissue contact may also be necessary along with additional safety protocols to ensure that autonomous operation can be done without the potential for additional patient risk.

VIII. Conclusion

In this paper, an estimation and control strategy for autonomous colonoscopy intervention on the REP is presented. Standard surgical tools can be used by the REP, and can be delivered robotically by the auto-feeding mechanism. The biopsy forceps are used as an example in this work, but other surgical tools can also be used after building their deflection models. The end position of the biopsy forceps is predicted by the workspace model, and the location of the target polyp center is estimated using the polyp position model. Both the REP motion control for tracking and capturing multiple views of the polyp and the REP pose adjustment control for colonoscopy intervention are proposed. With this strategy, the REP can

autonomously calculate the position of the polyp, adjust its posture and deliver a standard surgical tool to the polyp for intervention. The autonomous colonoscopy intervention experiments on a half colon simulator, a closed colon simulator and the MESA with haustral folds, demonstrate fast operation and good accuracy using this strategy.

While this work is the first study in autonomous colonoscopy intervention utilizing a mobile robotic endoscope, future work will focus on improving the accuracy of this method, robustly handling more complex and difficult polyp and endoscope positions and in ensuring the safety of the intervention, so as to allow for autonomous, accurate and fast colonoscopy interventions using a 1x robotic endoscope.

REFERENCES

[1] R. L. Siegel et al., "Colorectal cancer statistics, 2017," *CA: a cancer journal for clinicians*, vol. 67, no. 3, pp. 177-193, 2017.

[2] G. Iddan et al., ''Wireless capsule endoscopy,'' *Nature*, vol. 405, no. 6785, pp. 405–417, 2000.

[3] M. R. Yuce and T. Dissanayake, "Easy-to-swallow wireless telemetry," *IEEE Microwave magazine*, vol. 13, no. 6, pp. 90-101, 2012.

[4] P. Glass et al., "A Legged Anchoring Mechanism for Capsule Endoscopes Using Micropatterned Adhesives," *IEEE Trans. on Biomed. Engrg.*, vol. 55, no. 12, pp. 2759–67, Dec. 2008.

[5] P. Valdastri et al., "A New Mechanism for Mesoscale Legged Locomotion in Compliant Tubular Environments," *IEEE Transactions on Robotics*, vol. 25, no. 5, pp. 1047–57, Oct. 2009.

[6] D. Lee et al., "A simple and reliable reel mechanism-based robotic colonoscope for high mobility," *Proceedings of the Institution of Mechanical Engineers, Part C: Journal of Mechanical Engrg. Science*, vol. 232, no. 16, pp. 2753–63, Jul. 2017.

[7] P. Valdastri et al., "Magnetic air capsule robotic system: proof of concept of a novel approach for painless colonoscopy," *Surgical endoscopy*, vol. 26, no. 5, pp. 1238-1246, 2012.

[8] S. Yim et al., "Magnetically actuated soft capsule with the multimodal drug release function," *IEEE/ASME Transactions on Mechatronics*, vol. 18, no. 4, pp. 1413-1418, 2013.

[9] A. W. Mahoney and J. J. Abbott, "Generating Rotating Magnetic Fields with a Single Permanent Magnet for Propulsion of Untethered Magnetic Devices in a Lumen," *IEEE Transactions on Robotics*, vol. 30, no. 2, pp. 411–20, Apr. 2014.

[10] G. Pittiglio et al., "Magnetic Levitation for Soft-Tethered Capsule Colonoscopy Actuated With a Single Permanent Magnet: A Dynamic Control Approach," *IEEE Robotics and Automation Letters*, vol. 4, no. 2, pp. 1224-1231, 2019.

[11] D. Glozman et al., "A Self-Propelled Inflatable Earthworm-Like Endoscope Actuated by Single Supply Line," *IEEE Trans. on Biomed. Engineering*, vol. 57, no. 6, pp. 1264–72, Jun. 2010.

[12] C. C. Y. Poon et al., "Design of wormlike automated robotic endoscope: dynamic interaction between endoscopic balloon and surrounding tissues," *Surgical Endoscopy*, vol. 30, no. 2, pp. 772–8, May 2015.

[13] J. E. Bernth et al., "A Novel Robotic Meshworm with Segment-Bending Anchoring for Colonoscopy," *IEEE Robotics and Automation Letters*, vol. 2, no. 3, pp. 1718–24, Jul. 2017.

[14] D. Lee et al., "An elastic caterpillar-based self-propelled robotic colonoscope with high safety and mobility," *Mechatronics*, vol. 39, pp. 54–62, Nov. 2016.

[15] L. J. Sliker et al., "Surgical evaluation of a novel tethered robotic capsule endoscope using micro-patterned treads," *Surgical Endoscopy*, vol. 26, no. 10, pp. 2862–69, Apr. 2012.

[16] G. A. Formosa et al., "Novel Optimization-Based Design and Surgical Evaluation of a Treaded Robotic Capsule Colonoscope," *IEEE Transactions on Robotics (T-RO)*, vol. 36, no. 2, pp. 545-552, Oct. 2019. DOI: 10.1109/TRO.2019.2949466.

[17] K. Kong et al., "A rotational micro biopsy device for the capsule endoscope," in *Proc. IEEE /RSJ Intell. Robots Syst.*, 2005, pp. 1839–1843.

[18] S. Park et al., "A novel microactuator for microbiopsy in capsular endoscopes," *J. Micromechanics Microeng.*, vol. 18, no. 2, pp. 250–260, 2007.

[19] S. Yim et al., "Biopsy using a magnetic capsule endoscope carrying, releasing, and retrieving untethered microgrippers," *IEEE Transactions on Biomedical Engineering*, vol. 61, no. 2, pp. 513-521, 2013.

[20] D. Son et al., "Magnetically actuated soft capsule endoscope for fine-needle aspiration biopsy," in *2017 IEEE International Conference on Robotics and Automation (ICRA)*, 2017, pp. 1132-1139.

[21] S. P. Woods et al., "Wireless capsule endoscope for targeted drug delivery: mechanics and design considerations," *IEEE Transactions on Biomedical Engineering*, vol. 60, no. 4, pp. 945-953, 2012.

[22] D. L. Diehl et al., "Endoscopic retrieval devices." *Gastrointestinal endoscopy*, vol. 69, no. 6, pp. 997-1003, 2009.

[23] J. M. Prendergast et al., "A Platform for Developing Robotic Navigation Strategies in a Deformable, Dynamic Environment," *IEEE Robotics and Automation Letters (RA-L)*, vol. 3, no. 3, pp. 2670-77, Jul. 2018. DOI: 10.1109/LRA.2018.2827168.

[24] J. M. Prendergast et al., "Autonomous Localization, Navigation and Haustral Fold Detection for Robotic Endoscopy," in *IEEE/RSJ International Conference on Intelligent Robots and Systems (IROS)*, Madrid, Oct. 2018, pp. 783-790.

[25] G. A. Formosa et al., "A Modular Endoscopy Simulation Apparatus (MESA) for Robotic Medical Device Sensing and Control Validation," *IEEE Robotics and Automation Letters (RA-L)*, vol. 3, no. 3, pp. 4054-61, Oct. 2018. DOI: 10.1109/LRA.2018.2861015.

[26] R. Hartley and A. Zisserman, "Multiple View Geometry in Computer Vision," *Cambridge University Press*, p. 312, 2003.

[27] R. M. Summers, "Polyp size measurement at CT colonography: What do we know and what do we need to know?," *Radiology*, vol. 255, no. 3, pp. 707-720, 2010.